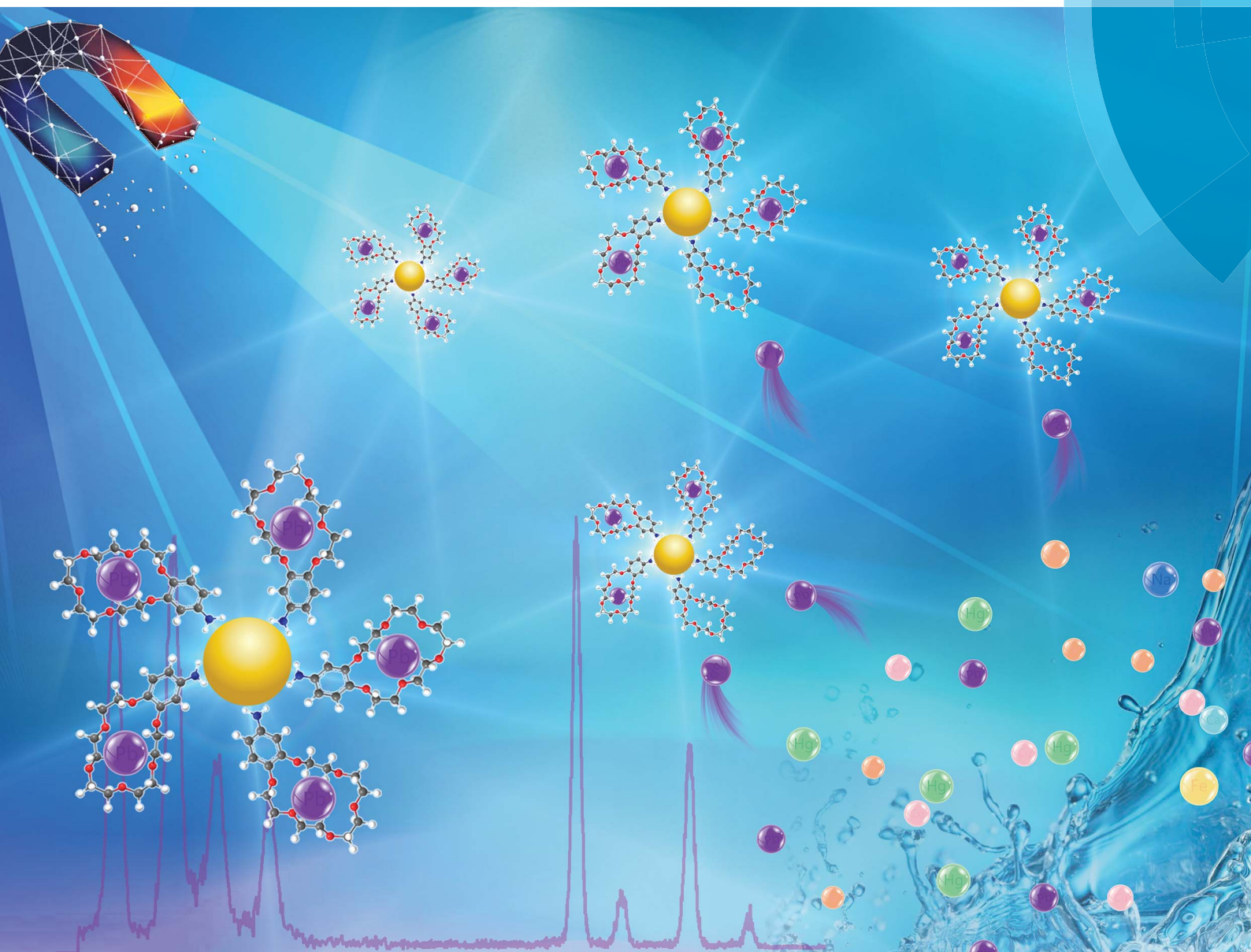


Analytical Methods

rsc.li/methods



ISSN 1759-9679



ROYAL SOCIETY
OF CHEMISTRY

Celebrating
IYPT 2019



PAPER

Yan-ping Shi *et al.*

4'-Aminobenzo-18-crown-6 functionalized magnetic nanoparticles as a solid-phase extraction adsorbent for the determination of Pb^{2+}

Cite this: *Anal. Methods*, 2019, 11, 1735

4'-Aminobenzo-18-crown-6 functionalized magnetic nanoparticles as a solid-phase extraction adsorbent for the determination of Pb²⁺†

Jing-yan Kang,^{ab} Wei Ha,^a Hai-xia Zhang ^c and Yan-ping Shi ^{*a}

A novel magnetic adsorbent has been designed and fabricated for the adsorption and determination of lead metal ions (Pb²⁺) based on a self-assembly approach between 4'-aminobenzo-18-crown-6 (AB18C6) and Fe₃O₄-CHO via dehydration condensation. 4'-Aminobenzo-18-crown-6 modified Fe₃O₄ (Fe₃O₄@AB18C6) was characterized by transmission electron microscopy (TEM), dynamic light scattering (DLS), Fourier transform infrared spectrometry (FT-IR), X-ray diffraction (XRD), vibrating sample magnetometry (VSM) and zeta potential analysis. Experiments proved that Fe₃O₄@AB18C6 had excellent adsorbability and selectivity for Pb²⁺, which is because the cavity of AB18C6 matches with the size of Pb²⁺. The magnetic solid-phase extraction (MSPE) method was applied for Pb²⁺ determination from tap water, rice, milk and apples. Furthermore, it was shown that the method had satisfactory linearity with a linear coefficient (*R*²) above 0.997, a linear range from 0.01 µg g⁻¹ to 10 µg g⁻¹, good precision with an RSD less than 8.62%, desirable recoveries ranging from 93.8% to 108.6%, and a low limit of detection (LOD) of 12.5 ng g⁻¹ for Pb²⁺. The established MSPE method has excellent potential for the selective determination of trace Pb²⁺ from complicated samples.

Received 18th December 2018

Accepted 1st March 2019

DOI: 10.1039/c8ay02760a

rsc.li/methods

Introduction

Heavy ion pollutants in food have aroused global attention because of their toxic and accumulative nature in humans, and they are a focus of the important global food contamination monitoring program of the United Nations Development Program (UNDP) and World Health Organization (WHO).^{1–3} Lead (Pb) is one of most prominent toxic heavy ions, and has a direct and adverse influence on human health even at trace concentrations.⁴ At present, there are some challenges to Pb²⁺ determination such as the matrix complexity of real samples and the fairly low concentration levels of Pb²⁺ in food samples.^{5,6} Various methods including X-ray fluorescence spectrometry (XRF),^{7,8} anodic stripping voltammetry (ASV)^{9,10} and inductively coupled plasma optical emission spectrometry (ICP-OES)^{11,12} have been reported for Pb²⁺ detection. Among these techniques, ICP-OES is popular because of its low cost, good stability, high accuracy and capacity for multielement

determination. However, Pb²⁺ determination in food samples with ICP-OES still suffers from interference by inorganic salts and other metal ions. Therefore, separation and enrichment steps are indispensable prior to trace determination of Pb²⁺ in complex real samples.

Various sample pretreatment methods have been developed for extraction of metal ions, such as liquid-liquid extraction (LLE),^{13,14} solid phase extraction (SPE),^{15,16} electromembrane extraction (EME),^{17,18} cloud point extraction (CPE)^{19,20} and magnetic solid-phase extraction (MSPE).^{21,22} MSPE technology has received considerable attention in recent years because it can combine extraction and separation, as well as elution and detection of analyte concentration, into one step.²³ In MSPE, the magnetic extraction materials can homogeneously disperse in solution and increase the interfacial area between adsorbents and analytes.²⁴ Compared with traditional centrifugation, magnetic adsorbents provide a more rapid and simpler method in the phase separation process.²⁵ Furthermore, the magnetic extraction materials can be reused after elution of analytes, which is economical and environmentally friendly.²⁶ Therefore, magnetic adsorbents exhibit many advantages for extraction such as rapidity, simplicity, excellent extraction capacity and selectivity. However, at present, there are some major challenges to adsorption of Pb²⁺ with MSPE: firstly, the trace levels of Pb²⁺ in samples require an effective MSPE method which has high extraction efficiency and good recovery. In addition, the complexities of real samples make it necessary for the extraction materials to have excellent selectivity and resistance to

^aCAS Key Laboratory of Chemistry of Northwestern Plant Resources, Key Laboratory for Natural Medicine of Gansu Province, Lanzhou Institute of Chemical Physics, Chinese Academy of Sciences, Lanzhou 730000, PR China. E-mail: shiyp@licp.cas.cn

^bUniversity of Chinese Academy of Sciences, Beijing 100049, PR China

^cCollege of Chemistry and Chemical Engineering, Lanzhou University, Lanzhou 730000, PR China

† Electronic supplementary information (ESI) available: Experimental method, characterization data, optimization of desorption conditions, and the determination of reuse times, and the linear relation of Pb²⁺ in data from different samples. See DOI: 10.1039/c8ay02760a

interference. Therefore, the design of an adsorbent with high extraction efficiency and good selectivity could improve the determination of Pb^{2+} in complex real samples and reduce tedious extraction times.²⁷

A functionalized magnetic adsorbent with high efficiency is crucial in MSPE technology to realize selectivity for the target, but it requires the modification of the magnetic materials with specific functional groups.²³ Various MSPE adsorbents have been prepared, including magnetic materials coated by inorganic complexes, grafted organic complexes, polymers and carbon nanomaterials (carbon nanotube and graphene).^{28–30} Among these magnetic materials, superparamagnetic iron-oxide nanoparticles are a novel material that is used for promoting the process of testing and realizing trace detection. Such nanoparticles can be applied in the enrichment and separation of trace metal ions, pesticides, and polycyclic aromatic hydrocarbons in food samples (milk, fruit, vegetables and cereals).^{31,32} For example, Bagheri *et al.* utilized molecularly imprinted polymers with propanamide as dummy template molecules and modified the surface of magnetic nanoparticles. The material was then applied for the accurate determination of acrylamide in food samples,³⁰ Ma *et al.* developed a MSPE technology using magnetic multi-walled carbon nanotubes as adsorbents, which realized the rapid determination of Hg^{2+} .³¹

18-Crown-6, a cyclic compound, more easily coordinates with metal ions than other single ligands as its oxygen atoms are all in the same plane and form a very strong negative potential barrier. Some studies have proved that 18-crown-6 and its derivatives can be applied in the adsorption of Pb^{2+} .³³ Fakhre and Ibrahim developed a novel supramolecular polysaccharide composite from cellulose and dibenzo-18-crown-6 using ceric ammonium nitrate as an initiator, and this had excellent adsorption capacity for heavy ions due to the dibenzo-18-crown-6.³⁴ Besides, Parra and his group reported a new material of multi-walled carbon nanotubes modified with benzo-18-crown-6 to realize the selection and detection of Pb^{2+} .³⁵ The 18-crown-6 derivative 4'-aminobenzo-18-crown-6 (AB18C6) has the negative cavity and the side chain of amidogen, which can not only coordinate with metal ions but can also be easily modified with the extraction medium. Above all, its cavity has the radius of 2.2–3.2 Å which exactly matches with the radius of Pb^{2+} (2.4 Å).³⁶ Thus AB18C6 is a suitable functionalized group which could realize the selective adsorption and determination of Pb^{2+} .

In this work, magnetic AB18C6 modified Fe_3O_4 nanoparticles ($\text{Fe}_3\text{O}_4\text{@AB18C6}$) were designed to develop a novel, simple and rapid method for the adsorption and detection of Pb^{2+} from different samples (tap water, apple, milk and rice). The method can not only realize the detection of trace Pb^{2+} with excellent selectivity, but also dramatically reduce the limit of detection (LOD). Moreover, a related MSPE procedure was established and the principal influencing factors including the content of AB18C6, solution pH, extraction time and salt concentration were optimized. In conclusion, the method was developed by combining it with ICP-OES and it was successfully applied for the detection of trace Pb^{2+} in real food samples.

Experimental

Materials

Standard solutions of lead ions, strontium ions, cobalt ions, cesium ions and barium ions (each at 1000 $\mu\text{g mL}^{-1}$) were purchased from National Standard Testing & Certification (Beijing, China). Manganese chloride, nickel chloride hexahydrate ($\text{NiCl}_2 \cdot 6\text{H}_2\text{O}$), sodium chloride (NaCl) and ethylene glycol $[(\text{CH}_2\text{OH})_2]$ were bought from Rionlon Bohua Pharmaceutical & Chemical Co., Ltd. (Tianjin, China). Glutaric dialdehyde, calcium chloride (CaCl_2) and copper chloride (CuCl_2) were purchased from Tianjin Kemiou Chemical Reagent Co., Ltd. (Tianjin, China). Zinc chloride (ZnCl_2), mercury dichloride (HgCl_2) and magnesium sulfate (MgSO_4) were bought from Xilong Scientific Co., Ltd. (Guangdong, China). Cerous nitrate was obtained from Sinopharm Chemical Reagent Co., Ltd. (Shanghai, China). Ferric chloride ($\text{FeCl}_3 \cdot 6\text{H}_2\text{O}$) was obtained from Beijing Tonghui Chemical Factory (Beijing, China). Sodium acetate (CH_3COONa) was bought from Kelong Chemical Reagent Factory (Chengdu, China). 1,6-Diaminohexane was obtained from Shanghai Chemical Reagent Co., Ltd. (Shanghai, China). Phosphate buffered saline was bought from Solarbio Science & Technology Co., Ltd. (Beijing, China). 4'-Nitrodibenzo-18-crown-6 was purchased from TCI Development Co., Ltd. (Shanghai, China). Sodium cyanoborohydride (NaBH_3CN) was obtained from J&K Scientific Co., Ltd. (Beijing, China). Trichloroacetic acid (TCA) was bought from Shanghai Shanpu Chemical Co., Ltd. (Shanghai, China). All reagents were of analytical grade and were used without further purification. Mixed working solutions were freshly prepared by diluting the stock solutions with deionized water to obtain the desired concentrations.

Synthesis of $\text{Fe}_3\text{O}_4\text{@AB18C6}$

The AB18C6 was synthesized according to the route shown in Fig. S1† and the $\text{Fe}_3\text{O}_4\text{@AB18C6}$ was prepared by a simple method according to previous reports, as shown in Fig. 1(a).²³ $\text{FeCl}_3 \cdot 6\text{H}_2\text{O}$ (1.0 g, 3.7 mmol) was dissolved in ethylene glycol (30 mL), and sodium acetate (2.0 g, 24.3 mmol) was gradually added into the solution which was constantly stirred for 30 min at room temperature. Eventually, 1,6-diaminohexane (0.65 g, 55.9 mmol) was added to the solution and the solution mixture was continuously stirred until a homogeneous and transparent solution was obtained. The solution was transferred into a Teflon-lined autoclave and reacted at 200 °C for 24 h. The magnetic nanoparticles were obtained, rinsed with water and ethanol for three times each, and then dried at 60 °C in a vacuum overnight.

The magnetic nanoparticles (200 mg) were dispersed in 60 mL of 0.01 mol L^{-1} phosphate buffer (PBS, pH: 7.4) *via* ultrasonication. Glutaric dialdehyde (20 mL) was added and the mixture was stirred for 10 h at room temperature. The resulting products ($\text{Fe}_3\text{O}_4\text{-CHO}$) were collected and washed with PBS solution to remove excess glutaric dialdehyde. Then the $\text{Fe}_3\text{O}_4\text{-CHO}$ was redispersed into 80 mL PBS solution, 4'-nitrodibenzo-18-crown-6 (800 mg) was added, and the reaction was allowed to continue for another 10 h at room temperature. Finally,

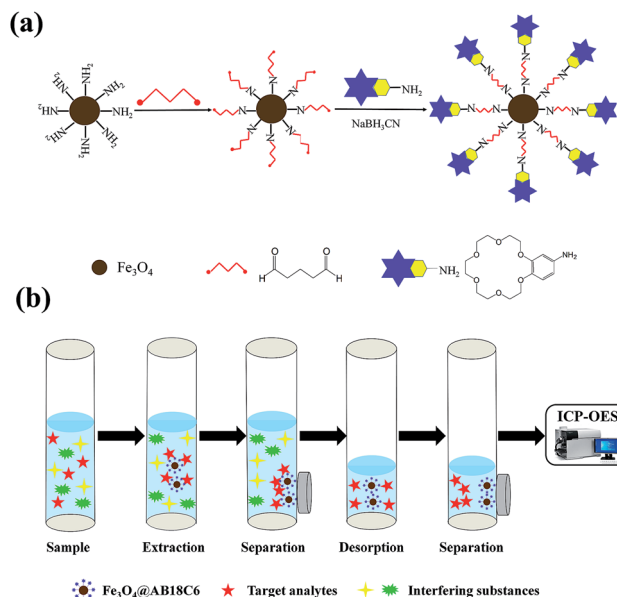


Fig. 1 Scheme showing the synthetic route for the preparation of $\text{Fe}_3\text{O}_4\text{@AB18C6}$ particles and their application for MSPE.

NaBH_3CN (0.6 g, 9.5 mmol) was added in order to reduce the unstable Schiff base and the solution was stirred for 10 h at 30 °C. The ultimate products ($\text{Fe}_3\text{O}_4\text{@AB18C6}$) were washed, collected and dried for further application.

Instrumentation

The concentrations of metal ions were determined using an Agilent Technologies 5100 inductively coupled plasma optical emission spectrometer (ICP-OES, Australia). Transmission electron microscopy (TEM) images were acquired using a Tecnai-G2-F30 field TEM instrument (FEI, USA). X-ray diffraction (XRD) patterns were observed on an X'pert PRO X-ray diffractometer using $\text{Cu K}\alpha$ radiation (Philips, Netherlands). Fourier transform infrared (FT-IR) spectra were obtained with an IFS120HR spectrometer (Bruker, Germany). The magnetic properties of the materials were analyzed using a 3473-70 vibrating sample magnetometry (VSM) instrument (Gmw Associates, USA). The zeta potentials and particle sizes of the materials were determined with a Zetasizer Nano series ZS instrument (Malvern Instruments, United Kingdom).

Magnetic solid-phase extraction and desorption

A schematic presentation of the MSPE procedure is shown in Fig. 1(b). $\text{Fe}_3\text{O}_4\text{@AB18C6}$ (5.0 mg) was dispersed into a 5.0 mL Pb^{2+} standard solution ($20.0 \mu\text{g mL}^{-1}$, pH: 5.0). Then the mixed solution was sonicated and shaken on an oscillator at room temperature for 60 min to achieve equilibrium. After that, the composite was gathered with an external magnet, and the supernatant solution was collected for extraction efficiency evaluation. Thereafter, the analytes adsorbed on the $\text{Fe}_3\text{O}_4\text{@AB18C6}$ composite were eluted by 1.0 mol L^{-1} HCl with ultrasound, and the $\text{Fe}_3\text{O}_4\text{@AB18C6}$ composite was magnetically collected from the desorption solution. The same desorption

procedure was repeated two more times. The resulting desorption solution was collected in a centrifuge tube for analysis.

Selectivity and anti-interference evaluation of $\text{Fe}_3\text{O}_4\text{@AB18C6}$

14 different individual metal ions solution, namely Na^+ , Ca^{2+} , Ce^{2+} , Cs^+ , Ba^{2+} , Co^{2+} , Mg^{2+} , Sr^{2+} , Mn^{2+} , Cu^{2+} , Hg^{2+} , Ni^{2+} , Fe^{3+} and Zn^{2+} , were prepared in deionized water such that each ion was at the concentration of $20 \mu\text{g mL}^{-1}$, and the solution pH was adjusted to 5.0. $\text{Fe}_3\text{O}_4\text{@AB18C6}$ (5.0 mg) was respectively dispersed into 5.0 mL of the solution of the 14 different individual metal ions and $20.0 \mu\text{g mL}^{-1}$ Pb^{2+} to evaluate the selectivity of the composite.

The mixture solution which simultaneously contained the metal ions of Na^+ , Ca^{2+} , Ce^{2+} , Cs^+ , Ba^{2+} , Co^{2+} , Mg^{2+} , Sr^{2+} , Mn^{2+} , Cu^{2+} , Hg^{2+} , Ni^{2+} , Fe^{3+} and Zn^{2+} and Pb^{2+} (each at $20.0 \mu\text{g mL}^{-1}$) was prepared and the pH was adjusted to 5.0. $\text{Fe}_3\text{O}_4\text{@AB18C6}$ (5.0 mg) was homogeneously dispersed into 5.0 mL of the solution above to evaluate the anti-interference properties of the composite.

Sample preparation

Apples were supplied by the local market of Lanzhou, China. Apple pieces (10.0 g) were accurately weighed into a juicer, juiced with 50 mL deionized water, transferred into a centrifuge tube and centrifuged at 4000 rpm for 20 min. Then, the supernatant was collected and the pH was adjusted to 5.0 for the MSPE of Pb^{2+} . Spiked samples were prepared through adding specific volumes of a standard solution of Pb^{2+} to the apple samples, and then the samples were prepared as described.

Milk was purchased from the local market of Lanzhou, China. Milk (200 mL) was transferred into a beaker and 10% trichloroacetic acid (TCA) was added dropwise until the protein was precipitated. The solution mixture was transferred into a plastic centrifuge tube and centrifuged at 4000 rpm for 20 min, the supernatant was collected and the pH was adjusted to 5.0. For the spiked samples, specific volumes of standard solutions of Pb^{2+} were added to the milk samples, and then the above preparation procedures were repeated.

Rice was bought from the market of Lanzhou, China. Rice samples were milled using an experimental miller, screened through a 65-mesh sieve and then used for subsequent experiments. Rice (10.0 g) was accurately weighed, mixed with 100 mL deionized water in a 250 mL beaker and sonicated for 2 h, and then the mixture was transferred into a centrifuge tube and centrifuged at 4000 rpm for 20 min. The supernatant was collected and the pH was adjusted to 5.0. Spiked samples were prepared through adding specific volumes of standard solutions of Pb^{2+} to the rice samples, and then the above preparation procedures were repeated.

Results and discussion

Characterization of $\text{Fe}_3\text{O}_4\text{@AB18C6}$

The morphologies of $\text{Fe}_3\text{O}_4\text{-NH}_2$ and $\text{Fe}_3\text{O}_4\text{@AB18C6}$ were investigated using TEM and DLS. The $\text{Fe}_3\text{O}_4\text{-NH}_2$ was

synthesized by a solvothermal reduction method, in which the electrostatic stabilization by NaAc and the high temperature of the reaction system prevented the nanoparticles from aggregating. It can be seen from Fig. 2(a) that the $\text{Fe}_3\text{O}_4\text{-NH}_2$ nanoparticles were mono-dispersed and the particle size was 163 nm, whereas the particle size was increased to 182 nm when AB18C6 was used to modify the surface of $\text{Fe}_3\text{O}_4\text{-NH}_2$, as shown in Fig. 2(b). The $\text{Fe}_3\text{O}_4\text{@AB18C6}$ obviously had good dispersity and the 4'-aminobenzo-18-crown-6 formed a thin film (19 nm); the $\text{Fe}_3\text{O}_4\text{@AB18C6}$ also retained the favorable dispersity during MSPE. After bound analytes were eluted from $\text{Fe}_3\text{O}_4\text{@AB18C6}$ by 1.0 mol L^{-1} HCl, the nanoparticles still retained their original morphologies, as revealed in Fig. 2(c), and they clearly remained stable. The EDS of $\text{Fe}_3\text{O}_4\text{-NH}_2$ and $\text{Fe}_3\text{O}_4\text{@AB18C6}$ are shown in Fig. S2;† the content of the elements C and O was increased in $\text{Fe}_3\text{O}_4\text{@AB18C6}$ which indicated that the AB18C6 had modified the surface of $\text{Fe}_3\text{O}_4\text{-NH}_2$.

The structure of $\text{Fe}_3\text{O}_4\text{@AB18C6}$ was further characterized by FT-IR spectroscopy. As shown in Fig. 3(a), the peak at 3420 cm^{-1} corresponding to the -CONH- bond existed in $\text{Fe}_3\text{O}_4\text{@AB18C6}$, which indicated that the dehydration condensation had occurred between -NH_2 of AB18C6 and -CHO of $\text{Fe}_3\text{O}_4\text{-CHO}$, and the peak at 2888 cm^{-1} belonging to the strong stretching vibration of $\text{-CH}_2\text{-}$ existed in both AB18C6 and $\text{Fe}_3\text{O}_4\text{@AB18C6}$. Besides, the peaks at 1626 cm^{-1} and 582 cm^{-1} could be attributed to the -NH_2 and Fe-O of $\text{Fe}_3\text{O}_4\text{-NH}_2$ respectively, and they also existed in $\text{Fe}_3\text{O}_4\text{@AB18C6}$. Moreover, some of the characteristic peaks of AB18C6 were also present in

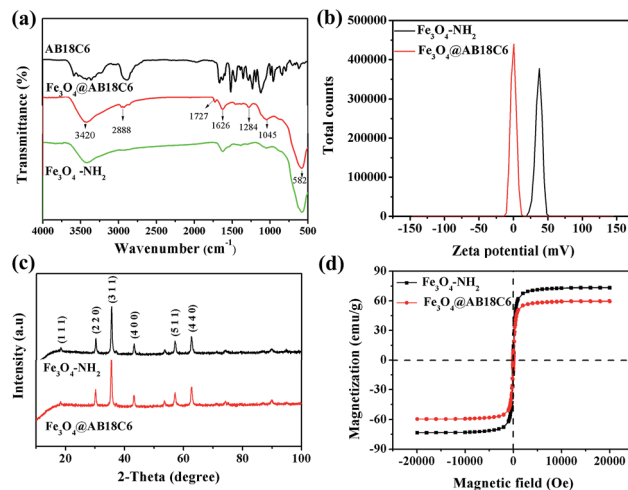


Fig. 3 (a) FT-IR spectra of AB18C6, $\text{Fe}_3\text{O}_4\text{-NH}_2$ and $\text{Fe}_3\text{O}_4\text{@AB18C6}$, (b) zeta potential of $\text{Fe}_3\text{O}_4\text{-NH}_2$ and $\text{Fe}_3\text{O}_4\text{@AB18C6}$, (c) XRD spectra of $\text{Fe}_3\text{O}_4\text{-NH}_2$ and $\text{Fe}_3\text{O}_4\text{@AB18C6}$, (d) magnetization curves of $\text{Fe}_3\text{O}_4\text{-NH}_2$ and $\text{Fe}_3\text{O}_4\text{@AB18C6}$.

the spectrum of the $\text{Fe}_3\text{O}_4\text{@AB18C6}$, such as the peak at 1727 cm^{-1} corresponding to the -NH_2 bond, and the peaks at 1284 cm^{-1} and 1045 cm^{-1} attributed to the -C-O-C- bond.^{28,30} All these data suggested that AB18C6 had modified the surfaces of $\text{Fe}_3\text{O}_4\text{-NH}_2$ successfully. To further prove the success of preparation of $\text{Fe}_3\text{O}_4\text{@AB18C6}$, the zeta potentials of $\text{Fe}_3\text{O}_4\text{-NH}_2$ and $\text{Fe}_3\text{O}_4\text{@AB18C6}$ were measured. As shown in Fig. 3(b), the zeta potential of $\text{Fe}_3\text{O}_4\text{@AB18C6}$ was negatively charged (-1.85 mV) and was obviously lower than that of $\text{Fe}_3\text{O}_4\text{-NH}_2$ (36.7 mV), because the -NH_2 of $\text{Fe}_3\text{O}_4\text{-NH}_2$ could combine with H^+ of H_2O and present a positive charge, however, when $\text{Fe}_3\text{O}_4\text{-NH}_2$ was modified with AB18C6, the AB18C6 prevented -NH_2 from interacting with H^+ of H_2O and AB18C6 had a zero charge. These results also suggested that $\text{Fe}_3\text{O}_4\text{-NH}_2$ had been successfully modified with AB18C6.

Identification of the crystalline phases of $\text{Fe}_3\text{O}_4\text{-NH}_2$ and $\text{Fe}_3\text{O}_4\text{@AB18C6}$ were performed by XRD analysis. As shown in Fig. 3(c), the XRD patterns of the $\text{Fe}_3\text{O}_4\text{@AB18C6}$ obviously exhibited characteristic diffraction peaks of Fe_3O_4 , displaying the diffraction peaks for the (111), (220), (311), (400), (511) and (440) planes, in accordance with those of the standard magnetite XRD pattern (JCPDS card, file no. 19-0629).²³ This showed that the composite structure of Fe_3O_4 was not destroyed by its functionalization.

Magnetism is an important feature of magnetic materials so VSM was conducted to ensure that the materials could be separated from a liquid medium in practical application. As shown in Fig. 3(d), the magnetic hysteresis loops for both $\text{Fe}_3\text{O}_4\text{-NH}_2$ and $\text{Fe}_3\text{O}_4\text{@AB18C6}$ showed almost zero coercivity and remanence, which suggested that the composites had excellent paramagnetism. The maximum saturation magnetization (M_s) values of $\text{Fe}_3\text{O}_4\text{-NH}_2$ and $\text{Fe}_3\text{O}_4\text{@AB18C6}$ were 72.9 emu g^{-1} and 59.4 emu g^{-1} , respectively. In comparison with $\text{Fe}_3\text{O}_4\text{-NH}_2$, $\text{Fe}_3\text{O}_4\text{@AB18C6}$ showed reduced magnetization, but the magnetic response of $\text{Fe}_3\text{O}_4\text{@AB18C6}$ was still sufficiently high for practical application.

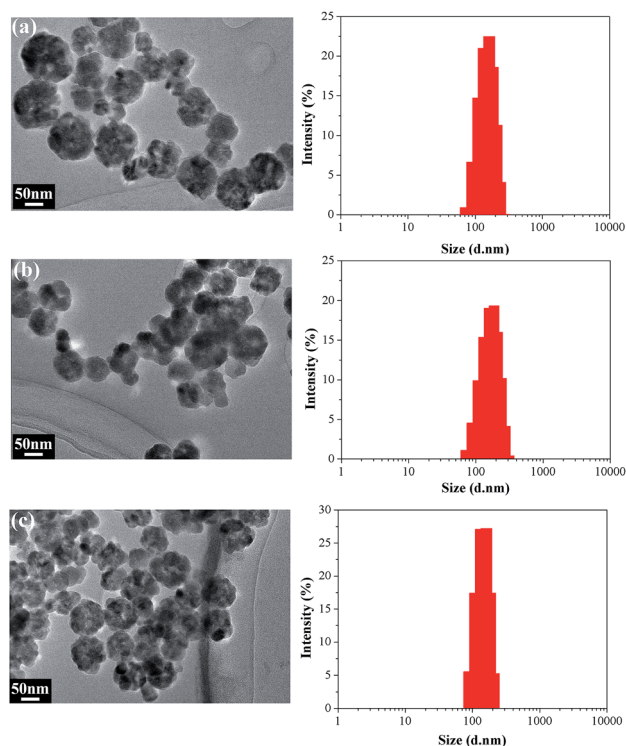


Fig. 2 TEM images and the corresponding DLS plots of (a) $\text{Fe}_3\text{O}_4\text{-NH}_2$, (b) $\text{Fe}_3\text{O}_4\text{@AB18C6}$ and (c) $\text{Fe}_3\text{O}_4\text{@AB18C6}$, after elution with 1.0 mol L^{-1} HCl.

Optimization of extraction parameters for MSPE

The extraction parameters are important for MSPE procedures, and greatly influence the extraction efficiency. Some vital extraction parameters for MSPE such as the pH, content of AB18C6, extraction time and salt concentration were evaluated.

The solution pH is closely linked to the properties of the analytes and the extractant, and influence the extraction efficiency.²⁷ The effect of the solution pH on MSPE was investigated by changing the pH from 3.0 to 8.0. The composite (5.0 mg) was added into the Pb^{2+} solution ($5.0 \mu\text{g mL}^{-1}$) at room temperature and incubated for 3 h without salt addition. Fig. 4(a) shows that the extraction efficiency was highest when the pH of the analyte solution was 5.0 and so the analyte solution was adjusted to pH 5.0 in the following experiments.

The content of AB18C6 is a relevant factor for the extraction system, because a limited amount of AB18C6 would reduce the adsorption capacity for Pb^{2+} , whereas excess AB18C6 could be wasteful. AB18C6 content was investigated by changing the ratio of $\text{Fe}_3\text{O}_4\text{-NH}_2$ to AB18C6 from 50 : 50 to 50 : 400, and then using 5.0 mg composite containing different quantities of AB18C6 for Pb^{2+} ($10 \mu\text{g mL}^{-1}$, pH: 5.0) extraction at room temperature without salt. As shown in Fig. 4(b), the extraction of Pb^{2+} was the highest when the ratio of $\text{Fe}_3\text{O}_4\text{-NH}_2$ to AB18C6 was 50 : 200. Therefore, the optimal quantity ratio of $\text{Fe}_3\text{O}_4\text{-NH}_2$ to ABA8C6 was 50 : 200 for MSPE.

Extraction time is connected with the extraction kinetics and the extraction equilibrium, which also influence the extraction efficiency.²⁶ Extraction times of 10–180 min were inspected for the MSPE of Pb^{2+} . The composite (5.0 mg) was added to Pb^{2+} solutions (each at $20 \mu\text{g mL}^{-1}$, pH: 5.0) and extraction was performed at room temperature without salt. As illustrated in Fig. 4(c), the extraction of Pb^{2+} was gradually increased as the extraction time increased from 10 min to 60 min, after which there was no obvious improvement in extraction, which suggested that the extraction equilibrium

had been attained. Thus 60 min was the optimal time for the MSPE of Pb^{2+} ions.

The salt concentration also influences the extraction efficiency by increasing the strength of solution ions and the viscosity of Pb^{2+} solution, and decreasing the solubility of analytes.²⁵ The influence of salt was investigated by adding a series concentration of sodium chloride to Pb^{2+} solution. The composite (5.0 mg) was employed for Pb^{2+} ($20 \mu\text{g mL}^{-1}$, pH: 5.0) extraction with different concentrations of added sodium chloride at room temperature. Fig. 4(d) shows that the extraction of Pb^{2+} decreased as the concentration of sodium chloride increased. Thus, salt addition reduced the MSPE of Pb^{2+} , and there was no need to add salt in subsequent extraction experiments.

Desorption conditions

Desorption is the other critical factor for MSPE, and it is also an important process for application in real samples.⁴⁰ Four acid solutions, namely hydrochloric acid, nitric acid, sulfuric acid and phosphoric acid, were selected for exploring the desorption conditions, as shown in Fig. S3(a).† The above desorption solvents were each employed three times to elute the extracted composite ($0.2 \text{ mL} \times 3$), and the results displayed that the hydrochloric acid had the highest desorption efficiency for Pb^{2+} , with a recovery attaining 100.3%. Then the concentration of hydrochloric acid was optimized: a series of hydrochloric acid concentrations was added to the extraction composite and each was used three times for desorption ($0.2 \text{ mL} \times 3$). As shown in Fig. S3(b),† when the concentration of hydrochloric acid was 1.0 mol L^{-1} , the desorption efficiencies were the highest. Therefore, 1.0 mol L^{-1} HCl was chosen as the desorption solvent for Pb^{2+} in this work.

Reusability evaluation

It is vital to evaluate the reusability of the MSPE composite. To evaluate the durability and reusability of the composite, the number of times that the extraction composite could be reused was investigated. The extraction composite was first desorbed, then cleaned by ultrapure water and dried, and the resulting composite was reused for the MSPE procedure. The result is shown in Fig. S4.† It was observed that the extraction capacity of the composite did not show any obvious loss after it was reused 3 times, which suggested that the composite was stable and that its structure was not changed by reuse. The FT-IR (Fig. S5†) and TEM (Fig. S6†) characterizations also displayed that the structure and morphology of $\text{Fe}_3\text{O}_4\text{@AB18C6}$ were stable after it was reused three times.

Selectivity and anti-interference evaluation

The selectivity and specificity of the composite in the MSPE experiment were evaluated by employing 14 metal ions which might appear in real samples. The experimental details are shown in Fig. 5(a). The metal ions, namely Na^+ , Ca^{2+} , Ce^{2+} , Cs^+ , Ba^{2+} , Co^{2+} , Mg^{2+} , Sr^{2+} , Mn^{2+} , Cu^{2+} , Hg^{2+} , Ni^{2+} , Fe^{3+} and Zn^{2+} , were employed for the MSPE procedure. The results clearly showed that the composite had excellent adsorption for Pb^{2+}

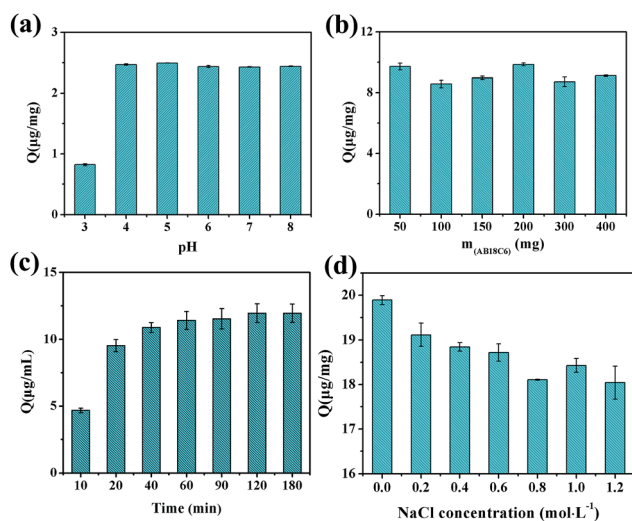


Fig. 4 Effect on Pb^{2+} extraction efficiency of (a) pH, (b) content of AB18C6, (c) extraction time, and (d) concentration of salt.

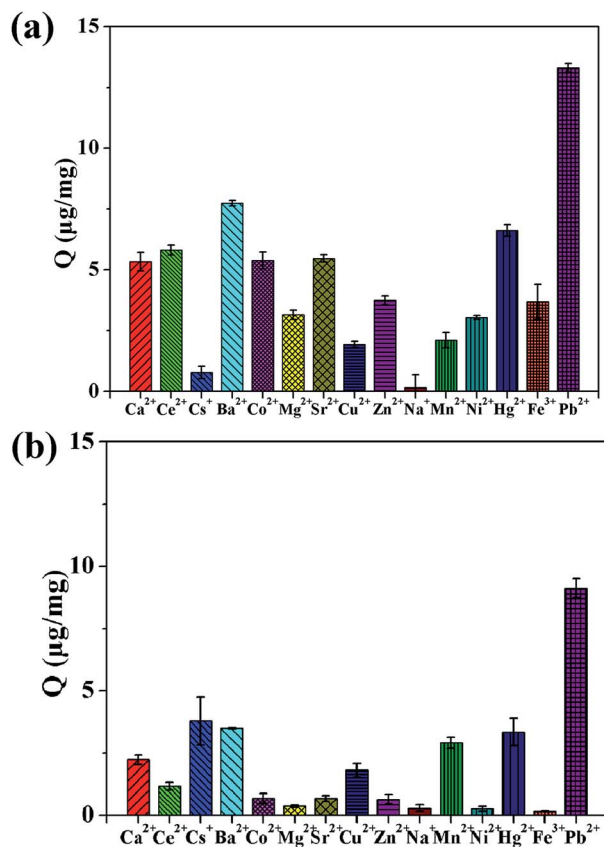


Fig. 5 (a) Selectivity and (b) anti-interference evaluation of $\text{Fe}_3\text{O}_4\text{@AB18C6}$ for Pb^{2+} extraction in a solution containing 14 other metal ions.

and that the adsorption capacity for Pb^{2+} was far more than that for the other metal ions. Furthermore, Fig. 5(b) exhibited that $\text{Fe}_3\text{O}_4\text{@AB18C6}$ had excellent anti-interference properties and that the existence of other interfering metal ions had little effect on the adsorption of Pb^{2+} in optimal conditions. This was attributed to three points: firstly, the AB18C6 was a cyclic compound, the oxygen atoms of AB18C6 were in the same plane and formed a strong negative potential barrier, so the compound easily coordinated with metal ions. Secondly, the AB18C6 had a hydrophobic exterior structure and hydrophilic interior, therefore it could form a stable coordination compound with Pb^{2+} . Lastly but not least, the AB18C6 cavity size matched the size of Pb^{2+} as well as provided ion-dipole interactions with the Pb^{2+} ion. In brief, the $\text{Fe}_3\text{O}_4\text{@AB18C6}$ exhibited ideal selectivity for Pb^{2+} because of the special structure of AB18C6.

Elucidation of adsorption and desorption mechanisms

With the purpose of evaluating the advantages of the proposed $\text{Fe}_3\text{O}_4\text{@AB18C6}$ -based MSPE and adsorption mechanism, different amounts of AB18C6-modified $\text{Fe}_3\text{O}_4\text{@AB18C6}$ were used to extract the same concentration of Pb^{2+} solution. As shown in Fig. 4(b), the adsorption capacity was the best when the ratio of $\text{Fe}_3\text{O}_4\text{-NH}_2$ to AB18C6 was 50 : 200. AB18C6 could be used to extract Pb^{2+} because it had special structure of

hydrophobic external skeleton and hydrophilic cavity.³⁷ Besides, the radius of AB18C6 cavity was 2.2–3.2 Å which exactly matched with the radius of Pb^{2+} (2.4 Å).³⁶ All these interactions contributed to the enhanced extraction affinity for Pb^{2+} and excellent selectivity for Pb^{2+} .

The desorption mechanism was mainly based on the pH of the analyte solution, which could affect the surface charge of AB18C6 and its ionization series. When the pH of the solution was low, the concentration of H^+ increased, which caused protonation of surface sites and increasing positive charges, and therefore, the adsorption capacity of $\text{Fe}_3\text{O}_4\text{@AB18C6}$ was reduced for positive metal ions (electrostatic repulsion).³⁸ In addition, the complexation of Pb^{2+} -AB18C6 and intermolecular association of H^+ -AB18C6 were in competition in acid solution.^{39,40} If the concentration of H^+ was at least 1.0 mol L^{-1} , the intermolecular association of H^+ -AB18C6 dominated, and the H^+ ions preferentially combined with AB18C6 and occupied the effective adsorption sites which had originally combined with Pb^{2+} . Therefore, as shown in Fig. S3,† the different acid solutions functioned as elution solutions and elution was best when the concentration of hydrochloric acid was 1.0 mol L^{-1} .

Method validation

The method for MSPE of Pb^{2+} was established according to the optimal conditions. In order to validate the performance of the method, a series of experiments to determine important analytical parameters such as linearity, accuracy, limit of detection (LOD) and limit of quantification (LOQ) was conducted.

Calibration curves for Pb^{2+} were established by extraction of solutions containing eight spiked levels of Pb^{2+} (0.01 $\mu\text{g g}^{-1}$, 0.1 $\mu\text{g g}^{-1}$, 0.5 $\mu\text{g g}^{-1}$, 1.0 $\mu\text{g g}^{-1}$, 4.0 $\mu\text{g g}^{-1}$, 6.0 $\mu\text{g g}^{-1}$, 8.0 $\mu\text{g g}^{-1}$, 10.0 $\mu\text{g g}^{-1}$) in three parallel experiments, as shown in Fig. S7.† Satisfactory linearity was obtained with the corresponding correlation coefficient (R^2) of 0.997 for Pb^{2+} , over the concentration range from 0.01 $\mu\text{g g}^{-1}$ to 10 $\mu\text{g g}^{-1}$. The LOD, defined as the concentration at a signal-to-noise ratio (S/N) of

Table 1 Analytical results for the determination of Pb^{2+} in apple, milk and rice samples ($n = 3$)

Sample	Spiked ($\mu\text{g g}^{-1}$)	Found ($\mu\text{g g}^{-1}$)	Recovery (%)	RSD (%)
Tap water	0	—	—	—
	0.1	0.111	111	5.41
	0.5	0.513	102	1.75
Apple	0	—	—	—
	0.1	0.104	104	5.08
	0.3	0.281	93.8	8.62
	0.5	0.486	97.2	1.09
Milk	0	—	—	—
	0.3	0.326	108	8.22
	0.5	0.512	102	5.24
Rice	0	—	—	—
	0.1	0.099	99.4	7.73
	0.3	0.321	107	8.62
	0.5	0.512	102	1.50

Table 2 Comparison of methods used for the determination of the target analytes^a

Extraction method	Analytical method	Matrix	Linearity	LOD	Recovery (%)	Interferences	Ref.
SPE	ICP-OES	Seafood	0.05–0.5 $\mu\text{g mL}^{-1}$	0.1 mg kg^{-1}	90–120	—	11
SPE	AAS	Water	0.2–50 $\mu\text{g L}^{-1}$	0.06 $\mu\text{g L}^{-1}$	95.5–104.6	7	15
UA-M-D- μSPE	FAAS	Water, fish, vegetables	2.0–600 $\mu\text{g L}^{-1}$	0.6 $\mu\text{g L}^{-1}$	92–97.6	—	41
MSPE	ICP-MS	Urine, plasma	—	0.157 $\mu\text{g L}^{-1}$	81–113	—	42
MSPE	FAAS	Water, fruit samples	3.5–150 $\mu\text{g L}^{-1}$	1.0 $\mu\text{g L}^{-1}$	94.0–106.0	—	43
MRT-SPE	UV-vis	—	0.01–0.75 mg L^{-1}	6.4 $\mu\text{g L}^{-1}$	—	4	44
MSPE	ICP-OES	Apple, milk and rice	0.01–10 $\mu\text{g g}^{-1}$	12.5 ng g^{-1}	93.8–108	14	This work

^a SPE: solid-phase extraction; MSPE: magnetic solid-phase extraction; MCSPE: microcolumn solid-phase extraction; UA-M-D- μSPE : ultrasound-assisted magnetic dispersive microsolid-phase extraction; MRT-SPE: molecular recognition technology solid-phase extraction.

3, was 12.5 ng g^{-1} , while that on the basis of an S/N ratio of 10 was 37.5 ng g^{-1} .

The calibration curves for Pb^{2+} in tap water, apple, milk and rice were established (Fig. S8, S9 and S10[†]) and the relevant parameters are listed in Table S1.[†] The results displayed that the curves were good even in the complex samples. The accuracy of the prepared method was validated by MSPE of water, apple, milk and rice samples spiked at three concentration levels (0.1 $\mu\text{g g}^{-1}$, 0.3 $\mu\text{g g}^{-1}$ and 0.5 $\mu\text{g g}^{-1}$) and the results are shown in Table 1. The extraction recoveries were used to evaluate accuracy. Recoveries ranged from 102% to 111% with the RSD in the range from 1.75% to 5.41% for tap water, from 93.8% to 104% with the RSD in the range from 1.09% to 8.62% for apple, from 102% to 108% with the RSD in the range from 5.24% to 8.22% for milk, and from 99.4% to 107% with the RSD in the range from 1.50% to 8.62% for rice. All these results illustrated that the proposed MSPE method for Pb^{2+} determination could satisfy the requirements of real sample analysis.

Precision

The precision of the proposed method was assessed by testing intra-day and inter-day variations. Both repeatability and intermediate precision were evaluated by analysis of five samples of tap water spiked at 0.5 $\mu\text{g g}^{-1}$. Repeatability was measured on the same day with the obtained RSD value of 1.89% while intermediate precision was measured on three consecutive days with RSD values of 4.24%.

Application to real sample analysis

To demonstrate the application of the prepared method, samples from apple, milk and rice purchased from a local market (Lanzhou, China) and tap water from our laboratory, were subjected to MSPE and ICP-OES analysis. The results indicated that Pb^{2+} was not detected in tap water, apple, milk or rice.

Method comparison

The proposed MSPE method was compared with some reported methods for Pb^{2+} determination, from the viewpoints of linearity, LOD, recovery and selectivity. As shown in Table 2, the prepared method had good extraction efficiency and the dispersive extraction mode compared well with other listed

methods. Furthermore, the proposed method exhibited a wide linearity range, desirable recovery and superior selectivity and anti-interference (as seen in Fig. 5). In addition, the magnetic extractant-based preparation method made the analysis procedure more convenient and time-saving. Due to the above discussed advantages, the proposed material can be considered as a promising extractant for Pb^{2+} determination from complex matrix samples.

Conclusions

A novel MSPE method was established for Pb^{2+} determination based on 4'-aminobenzo-18-crown-6 functionalized Fe_3O_4 ($\text{Fe}_3\text{O}_4\text{@AB18C6}$). Magnetic carrier technology made the separation procedure quick and convenient. The composite displayed excellent adsorption capacity and selectivity for Pb^{2+} , as the cavity of AB18C6 matched with the size of Pb^{2+} . Furthermore, the experimental parameters affecting adsorption efficiency were optimized, including the pH of solution, the content of AB18C6, the extraction time and the salt concentration. Under the optimal conditions, the established analytical method had good linearity, low limits of detection and satisfactory spiked recoveries when it was applied to trace Pb^{2+} determination. The results show that the proposed method can be applied to Pb^{2+} determination from complex matrix samples. Moreover, considering the trend in on-line MSPE determination of heavy metal ions in food samples, improved MSPE technology which can realize the automation of sample pretreatment will be researched in future work.

Conflicts of interest

There are no conflicts to declare.

Acknowledgements

This work was supported by the National Natural Science Foundation of China (Grant 21775153 and 21575150) and the National Key R&D Program of China (2017YFF0211100).

References

- 1 Z. O. Dada, *Environ. Int.*, 2006, **32**, 977.

- 2 P. N. Brandhoff, M. J. V. Bourgoniën, C. G. M. Onstenk, A. V. Avezathe and R. J. B. Peters, *Food Control*, 2016, **64**, 87.
- 3 H. S. Chiu, P. J. Huang, J. L. Wu and J. J. Wang, *Appl. Radiat. Isot.*, 2013, **81**, 356.
- 4 D. Ozdes, C. Duran, H. Bayrak, H. Serencam and H. B. Senturk, *J. Chil. Chem. Soc.*, 2013, **58**, 2204.
- 5 R. Hu, X. Wang, S. Dai, D. Shao, T. Hayat and A. Alsaedi, *Chem. Eng. J.*, 2015, **260**, 469.
- 6 J. Goel, K. Kadirvelu, C. Rajagopal and V. K. Garg, *J. Hazard. Mater.*, 2005, **125**, 211.
- 7 L. A. Hutton, G. D. O'Neil, T. L. Read, Z. J. Ayres, M. E. Newton and J. V. Macpherson, *Anal. Chem.*, 2014, **86**, 4566.
- 8 Y. Izumi, F. Kiyotaki, T. Minato and Y. Seida, *Anal. Chem.*, 2002, **74**, 3819.
- 9 D. H. Silva, D. A. Costa, R. M. Takeuchi and A. L. Santos, *J. Braz. Chem. Soc.*, 2011, **22**, 1727.
- 10 H. D. Vu, L. H. Nguyen, T. D. Nguyen, H. B. Nguyen, T. L. Nguyen and D. L. Tran, *Ionics*, 2014, **21**, 571.
- 11 É. J. Santos, A. B. Santos, A. B. Herrmann, S. Kulik, L. M. Baika, L. Tormen and A. J. Curtius, *Braz. Arch. Biol. Technol.*, 2013, **56**, 127.
- 12 S. Ozdemir, E. Kilinc, K. S. Celik, V. Okumus and M. Soylak, *Food Chem.*, 2017, **215**, 447.
- 13 M. Lamsayah, M. Khoutoul, A. Takfaoui and R. Touzani, *Cogent Chem.*, 2016, **2**, 1230359.
- 14 U. Domańska and A. Rękawek, *J. Solution Chem.*, 2009, **38**, 739.
- 15 X. Q. Cai, J. H. Li, Z. Zhang, F. F. Yang, R. C. Dong and L. X. Chen, *ACS Appl. Mater. Interfaces*, 2014, **6**, 305.
- 16 M. Eftekhari, M. Gheibi, M. Akrami and F. Iranzad, *New J. Chem.*, 2018, **42**, 1159.
- 17 M. Silva, C. Mendiguchia, C. Moreno and P. Kuban, *Electrophoresis*, 2018, **39**, 2152.
- 18 P. Kuban, L. Strieglerova, P. Gebauer and P. Bocek, *Electrophoresis*, 2011, **32**, 1025.
- 19 K. Pytlakowska, V. Kozik and M. Dabioch, *Talanta*, 2013, **110**, 202.
- 20 R. E. Babiker and M. A.-Z. Eltayeb, *Am. J. Chem.*, 2018, **8**, 51.
- 21 M. Hemmati, M. Rajabi and A. Asghari, *Microchim. Acta*, 2018, **185**, 160.
- 22 R. Yi, G. Ye, F. C. Wu, D. Lv and J. Chen, *J. Radioanal. Nucl. Chem.*, 2015, **308**, 599.
- 23 N. Li, J. Chen and Y. P. Shi, *Anal. Chim. Acta*, 2017, **949**, 23.
- 24 A. Amiri, M. Baghayeri and M. Sedighi, *Mikrochim. Acta*, 2018, **185**, 393.
- 25 J. P. Ma, G. Wu, Sh. Li, W. Q. Tan, X. Y. Wang, J. H. Li and L. X. Chen, *J. Chromatogr. A*, 2018, **1553**, 57.
- 26 W. K. Li, H. X. Zhang and Y. P. Shi, *Anal. Chim. Acta*, 2018, **1011**, 40.
- 27 M. Hemmati, M. Rajabi and A. Asghari, *Microchim. Acta*, 2018, **185**, 160.
- 28 W. K. Li, H. X. Zhang and Y. P. Shi, *J. Chromatogr. B: Anal. Technol. Biomed. Life Sci.*, 2017, **1059**, 27.
- 29 N. Li, J. Chen and Y. P. Shi, *J. Chromatogr. A*, 2016, **1441**, 24.
- 30 A. R. Bagheri, M. Arabia, M. Ghaedi, A. Ostovana, X. Y. Wang, J. H. Li and L. X. Chen, *Talanta*, 2019, **195**, 390.
- 31 J. P. Ma, L. H. Jiang, G. G. Wu, Y. Xia, W. H. Lu, J. H. Li and L. X. Chen, *J. Chromatogr. A*, 2016, **1466**, 12.
- 32 S. F. Xu, L. X. Chen, J. H. Li, Y. F. Guan and H. Z. Lu, *J. Hazard. Mater.*, 2012, **237–238**, 347.
- 33 S. Dernini, A. Scrgugli, S. Palmas and A. M. Polcaro, *J. Chem. Eng. Data*, 1996, **4**, 1388.
- 34 N. A. Fakhre and B. M. Ibrahim, *J. Hazard. Mater.*, 2018, **343**, 324.
- 35 E. J. Parra, P. Blondeau, G. A. Crespo and F. X. Rius, *Chem. Commun.*, 2011, **47**, 2438.
- 36 Y. C. Qian, Zh. Zhang, W. Tian, L. P. Wen and L. Jiang, *Faraday Discuss.*, 2018, **210**, 101.
- 37 G. W. Gokel, W. M. Leevy and M. E. Weber, *Chem. Rev.*, 2004, **104**, 2723.
- 38 F. F. Bai, C. S. He, G. J. Chen, J. C. Wei, J. C. Wang and G. Ye, *Energy Procedia*, 2013, **39**, 396.
- 39 T. Tachibana, Y. Wu, H. Mimura and Y. Niiboria, *J. Ion Exch.*, 2007, **18**, 384.
- 40 E. Blasius, W. Klein and U. Schon, *J. Radioanal. Nucl. Chem.*, 1985, **89**, 389.
- 41 B. Fahimirad, A. Asghari and M. Rajabi, *Microchim. Acta*, 2017, **184**, 3027.
- 42 J. P. Sun, Q. L. Liang, Q. Han, X. Q. Zhang and M. Y. Ding, *Talanta*, 2015, **132**, 557.
- 43 A. A. Asgharinezhad, M. Rezvani, H. Ebrahimzadeh, N. Shekari, N. Ahmadinasab and M. Loni, *Anal. Methods*, 2015, **7**, 10350.
- 44 I. M. M. Rahman, Y. Furusho, Z. A. Begum, R. Sato, H. Okumura, H. Honda and H. Hasegawa, *Cent. Eur. J. Chem.*, 2013, **11**, 672.